Journal of Solid State Chemistry 184 (2011) 1540–1544

Contents lists available at ScienceDirect

Journal of Solid State Chemistry

journal homepage: www.elsevier.com/locate/jssc

Preparation of blue-emitting $CaMgSi_2O_6:Eu^{2+}$ phosphors in reverse micellar system and their application to transparent emissive display devices

Sungho Choi [a,*], Se-Won Tae [b], Jung-Hyun Seo [a,c], Ha-Kyun Jung [a]

[a] Device Materials Research Center, Korea Research Institute of Chemical Technology, P.O. Box 107, Yuseong, Daejeon 305-600, Republic of Korea
[b] Seoul Semiconductor, Wonsi-dong, Danwon-gu, Ansan-city, Gyeonggi-do, Republic of Korea
[c] Department of Materials Science and Engineering, Korea University, Anam-dong, Seoul, Republic of Korea

ARTICLE INFO

Article history:
Received 9 March 2011
Received in revised form
13 April 2011
Accepted 17 April 2011
Available online 27 April 2011

Keywords:
Nanophosphor
Luminescence
Reverse micelle
Transparent device

ABSTRACT

Blue-emitting Eu^{2+}-doped $CaMgSi_2O_6$ phosphors were prepared by the reverse micelle method. The resultant particles were nanocrystalline with a grain size of about <300 nm and exhibited a characteristic blue emission spectrum centered at 445 nm induced by the oxygen coordinated Eu^{2+} ions. By using the corresponding nanophosphors followed by the formation of a uniform phosphor layer, we have demonstrated the mini-sized transparent plasma-discharge panels and investigated their luminance characteristics. Phosphor coated panel is properly transparent, $\geq 65\%$, at the visible wavelength region and illuminates a characteristic blue emission under Ne/Xe plasma discharge conditions. Thus, we can obtain a fast decaying, robust blue-emitting silicate phosphor layer under excited plasma radiation for upcoming emissive display devices like as transparent and three-dimensional plasma display panels.

1. Introduction

Multi-function, flexibility, and transparency are among the important features that are demanded for upcoming display devices. Recently, transparent devices attracted much attention in display applications such as car navigation systems and decoration lighting devices. Using vacuum processed inorganic thin film phosphors, the electroluminescent (EL) device has become the first transparent display device [1]. Very recently, transparent displays have been demonstrated mainly in the field of organic light-emitting devices [2]. Even though those proposed devices suggest a possible approach to the realization of transparent displays, the development of devices with high luminance, good transparency, and vivid image is still needed. Thus, the emissive display devices are considered as the other promising candidates to meet those requirements.

To date, plasma display panels (PDPs) are regarded as one of the most cost effective display devices in the area of large-area flat panel displays (FPDs) [3]. PDPs, good color purity with wide-ranging viewing angles, used a vacuum ultraviolet (VUV) illumination generated by plasma discharge as the excitation source of red-, green-, and blue-emitting phosphors [4]. Synthesis and luminescent properties of inorganic phosphors have been extensively investigated for recently developed FPDs [5]. The transparency of conventional PDPs, as usual, is confined principally by the use of micron-scaled phosphors that exhibit considerable light scattering. However, by introducing nanoscale phosphors for the formation of scattering-free/-less luminescent layers, the transparent displays based on the plasma discharge-driven technology came to be realized.

There has been much recent interest in the preparation and properties of nanoparticles [6–8]. While the optical properties of quantum dots are governed by size-dependent quantum confinement, the luminescence behaviors of, for example, rare earth or transition metal ion activated oxide nanophosphors are rarely dependent on particle size. Thus, as mentioned before, by using the shape and size controlled nanophosphors with comparable emission properties under the given excitation conditions, transparent luminescent layers can be achieved.

The preparation method using small water pools in reverse micelles as the reaction media has been studied for preparing various metal oxide nanoparticles [9–11]. One of the advantages of this method is that localized super saturation of the reactants is suppressed and a uniform nucleation occurs since the reactants are dispersed very well in the reverse micellar solution. In addition, the reverse micelles can protect the nanoparticles against excess aggregation.

Rare-earth ion-doped alkaline earth silicate phosphors have attracted interest because of their high luminescence efficiency and chemical stability. Among these, Eu^{2+}-doped $CaMgSi_2O_6$ (CMS) has been considered one of the most promising blue-emitting phosphors for PDPs [12]. This phosphor has been developed to overcome the drawbacks of the conventional blue

* Corresponding author. Fax: +82 42 861 4151.
E-mail address: shochoi@krict.re.kr (S. Choi).

0022-4596/$ - see front matter © 2011 Elsevier Inc. All rights reserved.
doi:10.1016/j.jssc.2011.04.032

phosphor, $BaMgAl_{10}O_{17}:Eu^{2+}$ (BAM), which undergoes degradation by ion bombardment or ultraviolet radiation [13,14]. In addition, Eu^{2+}-doped CMS can also be used as a long phosphorescent phosphor when co-doped with Dy^{3+} [15]. There are various methods to produce efficient rare-earth ion doped CMS phosphors, such as the solid-state reaction method, sol–gel process, and spray pyrolysis [16–18]. However, the resultant particles were usually microscale and irregular in shape, making them unsuitable for transparent luminescent layers, as we mentioned before. Therefore, finer nanophosphors with low scattering loss in a visible wavelength region are desired for uniform luminescence under specific excitation conditions. Additionally, low crystallinity, surface defects and low production yield should be overcome in the preparation of highly efficient nanoscale phosphors.

In this paper, we synthesized Eu^{2+} doped CMS nanophosphors by using the reverse micelle method. Phase formation, particle morphology, and photoluminescent properties of the resultant nanoparticles were thoroughly investigated. Using the stable colloidal solutions, a transparent blue-emitting phosphor layer was successfully formed on a glass plate and a mini-sized plasma discharge operated transparent panel was demonstrated. Our results demonstrate that moderate particle size and illumination under excited plasma radiation can be combined to yield an ideal phosphor layers for use in transparent PDPs.

2. Experimental

Eu^{2+} doped CMS nanophosphors were prepared by a reverse micelle method. The starting materials were cyclohexane (Samchun, 99.5%), polyoxyethylene (5) nonylphenylether (Igepal CO-520, Aldrich, 98%), tetraethylorthosilicate (TEOS, Aldrich, 98%), and reagent grade metal chlorides: $CaCl_2$ (Aldrich, 99+%), $MgCl_2$ (Aldrich, 99.995%), $EuCl_2$ (Aldrich, 99.9%), respectively. Firstly, two individual stock solutions were prepared: the first one (S1) contained 10 ml of cyclohexane mixed with 1.67 g of TEOS and 4.01 g of Igepal. The second mixture (S2) was the stoichiometric amount of metal chloride dissolved water: 0.5587 g of $CaCl_2$, 0.8132 g of $MgCl_2$, and 0.0733 g of $EuCl_2$, in 2 ml of deionized water. The concentration of Eu was 0.01 of molar ratio. Initially, the two separate micelles above were prepared by thorough homogenization. Then S2 solution was added to the S1 stock solution very slowly with vigorous stirring at 400 rpm and mixing for 1 h. Finally, 5 ml of NH_4OH (Junsei, 28%) was added drop-by-drop to the resultant mixed solution. After stirring for 30 min, the obtained white precipitates were then centrifuged, followed by washing several times using ethanol. Those as-prepared precipitates were dried at 80 °C for 24 h and fired at 1000 °C for 3 h under air ambient. After firing, the obtained powders were ground and then reheated in a reducing atmosphere of N_2–H_2 (2%) at 1100 °C for 3 h.

In order to prepare a coating solution, 0.05 g of the as-prepared Eu^{2+} doped CMS nanopowders were agitated with a sonic dismembrator (Fisher Scientific) in 0.3 g of polyvinylpyrrolidone (Aldrich, 99%) dissolved 10 ml of 2-methoxyethanol for 10 min. Using a spin-casting method (2000 rpm, 30 s), a luminescent layer was formed on a 6×9 cm^2 sized glass plate. After coating, the films were dried at 300 °C for 10 min. The above coating process was repeated several times to obtain a layer with the desired thickness. Post annealing was conducted at 400 °C for 10 h in order to remove any residual polymeric agents.

The luminescence behavior of the nanophosphor-coated layer was investigated by using mini-sized ac-plasma discharge driven test panels. The front side consisted of a glass substrate, electrodes, a dielectric layer, and MgO thin film. It was then combined with the nanophosphor-coated rear plate with a gap of 100 μm and filled with a Ne–20% Xe discharge gas mixture of 400 Torr. In order to perform discharge tests on the fabricated panels, a conventional pulsed AC power supply was used with a frequency of 30 kHz and a voltage of 290 V in order to initiate the glow discharge of mini-sized test panels.

Phase formation and crystallinity of as-prepared nanophosphors were examined by using a Rigaku DMAX-33 X-ray diffractometer (XRD) with Cu$K\alpha$ radiation. The particle morphology, size, and crystallinity were analyzed by field emission-scanning electron microscopy (FE-SEM, Philips XL-30S) and transmission electron microscopy (TEM, JEOL 200CX). The vacuum ultraviolet photoluminescence (VUV-PL) spectra of the nanophosphors were measured using a deuterium lamp equipped vacuum chamber by scanning the wavelength between 350 and 650 nm. The luminescence decay curves were obtained by a digital oscilloscope (Tektronix DPO 3014) using a xenon flash lamp as an excitation source. UV–visible spectroscopy (Shimadzu, UV-2450) was used to measure the transmittance of deposited nanophosphor layers. The luminance of the fabricated transparent mini-sized test panels was measured with a spectroradiometer, Minolta CS-1000.

3. Results and discussion

A typical XRD pattern of the undoped and Eu^{2+} doped CMS nanoparticles synthesized by the reverse micelle method, followed by firing, as presented in Fig. 1(a) and (b), shows that the as-prepared particles are well-crystallized with phase pure compound. The diffraction patterns matched to the reference JCPDS card of $CaMgSi_2O_6$ (no. 98-000-0197, Fig. 1(d)), having a monoclinic phase with a $C2/c$ space group. All the peaks can be indexed to the monoclinic phase, indicating that the doping ion, Eu^{2+}, did not form other additional phases in the synthesis process. Note that the Eu^{2+} activator concentration of reverse micellar grown CMS phosphors we made is about 1 mol% of ratio based on the our previous work, which leads to the optimum luminescence efficiency [18].

We can realize that the XRD patterns of reverse micellar grown Eu^{2+} doped CMS are in good agreement with samples prepared from other synthetic methods like as solid-state reaction, sol–gel and spray pyrolysis [15–18]. When the particles are formed out of the controlled synthetic conditions, however, a subsidiary phase denoted as *, $MgSiO_3$ (JCPDS no. 01-076-0490, Fig. 1(e)) can be detected, as shown in Fig. 1(c). That is to say, the vigorous mixing of the metal ion solution with surfactant dissolved organic solvent is likely to cause an aggregation of nanoparticles and/or prevent forming the homogeneous aqueous solution during the sedimentation. With an increase of the firing temperature up to 1100 °C,

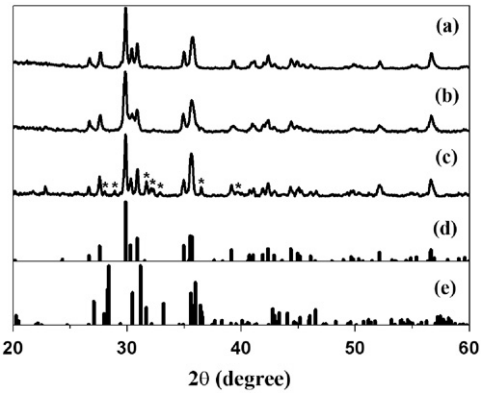

Fig. 1. XRD pattern of (a) $CaMgSi_2O_6$ particles, (b) Eu^{2+}-doped $CaMgSi_2O_6$ particles, and (c) Eu^{2+}-doped $CaMgSi_2O_6$ particles presented with subsidiary $MgSiO_3$ (denoted as *) phase. Reference diffraction patterns of (d) $CaMgSi_2O_6$ compound (JCPDS no. 98-000-0197) and (e) $MgSiO_3$ compound (JCPDS no. 01-076-0490).

another silicate phase, $Ca_2MgSi_2O_7$, was appeared, and the luminescence efficiency gradually decreased under excited plasma radiation.

The FE-SEM image for the Eu^{2+} doped CMS particle thus prepared is shown in Fig. 2(a). According to the SEM images, the as-synthesized CMS particle size was 200–300 nm with largely aggregated spherical shaped particles. Nonetheless, we were able to prepare a coating solution with dispersed nanoparticles for the luminescent film layer with the help of mild sonication to pulverize the aggregated primary particles. The corresponding TEM images are presented in Fig. 2(b) and (c). The obvious lattice spacing in the high-resolution (HR) TEM image (Fig. 2(c)), exhibited high crystallinity and phase pure CMS nanoparticles [19]. Thus, we can realize that the crystalline Eu^{2+} activated CMS with a size of about 200–300 nm particles can be successfully obtained by the reverse micelle solution at an appropriate acidity.

Fig. 3 shows normalized PL emission spectra of the Eu^{2+} activated CMS phosphor prepared by the reverse micelle method and commercial Eu^{2+} activated $BaMgAl_{10}O_{17}$ (BAM) purchased from Phosphor Technology, Inc. The emission of Eu^{2+} activated CMS nanophosphor (Fig. 3(b)), exhibited an intense blue emission with a relatively narrow band spectrum under excited 147 nm VUV radiation than the Eu^{2+} activated BAM blue phosphor (Fig. 3(a)). The full width at half maximum (FWHM) of CMS phosphors was 42 nm, while that of the BAM was 60 nm, thereby improving the color chromaticity although the spectral positions are identical. The emission band positioned at 450 nm, which is due to the 4*f*–5*d* transition of Eu^{2+} ion substituted by a six-fold oxygen coordinated Ca^{2+} site similar to that of the solid state reaction prepared CMS phosphor [15].

Fig. 4 monitored the afterglow decay curve of CMS phosphors, which were irradiated by using 147 nm as light source. For comparison, that of commercial Eu^{2+} activated BAM phosphors is also presented. Upon luminescence decaying, the experiment data match well with the single exponential function, $I(t)=I_o+A\exp(-t/\tau)$, where $I(t)$ and I_o describe the fluorescence intensities, A represents the pre-exponential factor, and τ denotes the luminescent lifetime constant. We can realize that τ for Eu^{2+} doped CMS nanophosphor and the commercial Eu^{2+} activated BAM phosphor is exactly same, ~0.32 ms.

Jung et al. [18] prepared $CaMgSi_2O_6$:Eu^{2+} phosphor via the spray pyrolysis method to examine the thermal stability. The color shift was not observed after the film-making process, and the reduction of the emission intensity was small compared to the case with blue-emitting BAM phosphors. In addition, the maximum PL intensity of the Eu^{2+} doped CMS particles was very similar to that of the BAM phosphor. Therefore, we can expect good thermal degradation behavior in reverse micellar grown CMS nanophosphor with comparable fast decaying property similar to the Eu^{2+} activated BAM phosphor.

According to past research, afterglow is determined by released holes from the traps in the host lattices. The afterglow time of phosphors was considerably influenced by the depth of the trap level which was dominated by the activating rare earth ions [17]. Recently, it has become accepted that the phosphors used for on-going 3D and high-definition (HD) PDPs should have fast response so that there is no lag in image transformation.

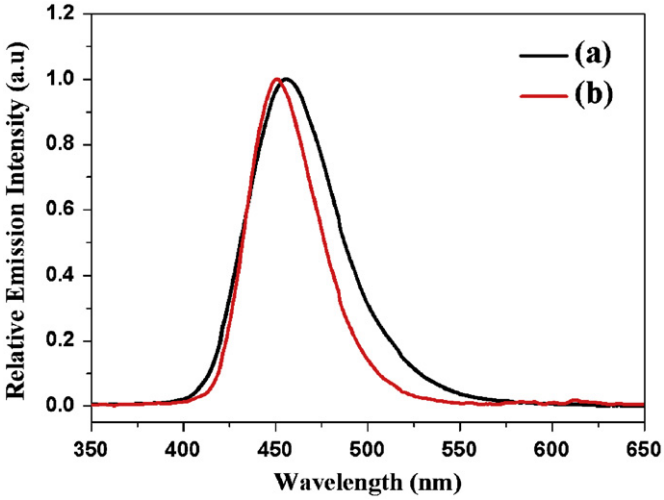

Fig. 3. VUV-emission spectrum of the commercial micronsized Eu^{2+} activated $BaMgAl_{10}O_{17}$ (a) and Eu^{2+}-activated $CaMgSi_2O_6$ particles prepared by a reverse micelle method (b). Both samples are measured under excited 147 nm radiations.

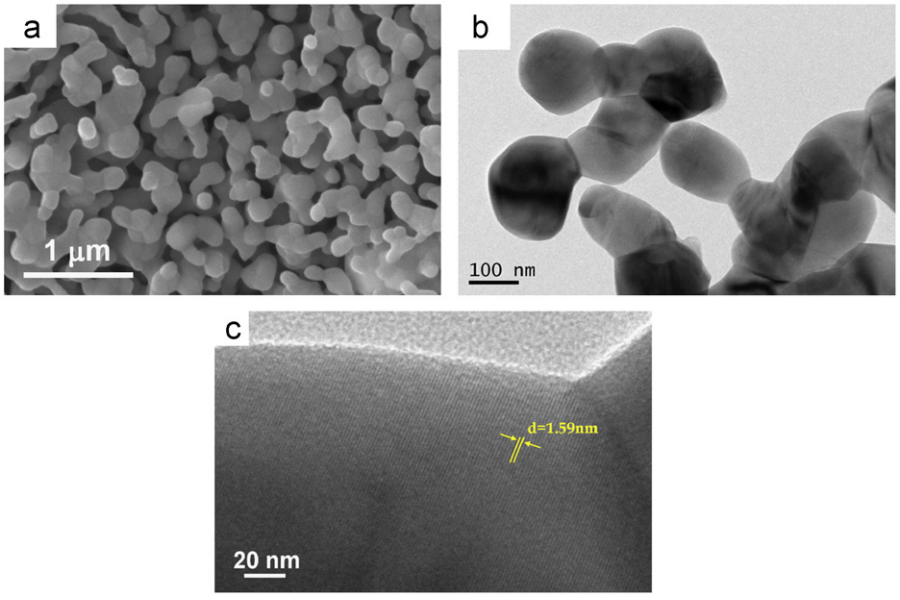

Fig. 2. (a) FE-SEM image of the as-synthesized Eu^{2+}-doped $CaMgSi_2O_6$ particles. (b) and (c) TEM images of the corresponding phosphor particles.

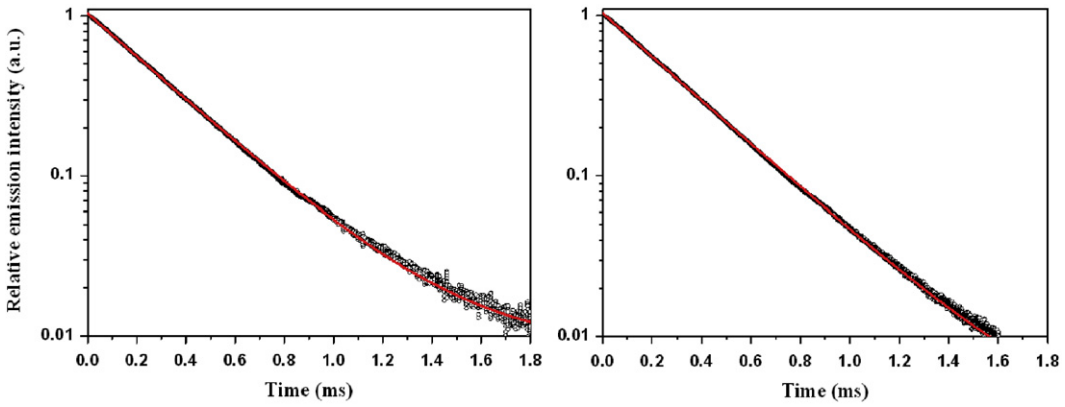

Fig. 4. Luminescence decay of the reverse micellar grown Eu^{2+}-doped $CaMgSi_2O_6$ particles (left) and commercial Eu^{2+} activated $BaMgAl_{10}O_{17}$ phosphor (right) under excited 147 nm radiations. Fitted data are shown as red lines. (For interpretation of the references to color in this figure legend, the reader is referred to the web version of this article.)

The ideal decay time of phosphor suitable for glass-type 3D displays should be less than $\tau_{1/10} < 2$ ms to prevent cross-talk-induced ghost images [20]. Additionally, particle size and excitation-energy-dependent luminescence spectral changes in nanoscale phosphors were previously reported [21,22]. In the case of hydrothermally grown Eu^{3+}-activated nanophosphors, the local environments for the activators in/near the surface are easily rearranged by different external radiation energy because of the remnant surface defects. The fluorescence decay time of the colloidal nanophosphors exponentially decreases with a decrease in the particle sizes attributed to high surface-to-volume ratio. Therefore, the correlation of the luminescence decay with particle size should be considered; even the Eu^{2+} activated BAM phosphor normally has fast decaying behaviors under excited plasma discharge conditions. Based on our results, we can realize that the afterglow feature of Eu^{2+}-activated CMS prepared by the reverse micelle method normally results from the 5*d*–4*f* typical electric dipole transition produced by incorporated Eu^{2+} irrespective of the surface induced non-radiative transitions.

One of the ideal forms of upcoming display devices like TVs would be transparent devices that only show up when in use. This type of technology could create an emissive display embedded into the windshield of a car or device modules so that one could obtain information without having to take his or her eyes off of the real concerns.

Such a good transparency is also confirmed by the readability of some characters through the reverse micellar grown nanophosphor layer coated glass shown in the inset image of Fig. 5. The optical transmittance of the resultant nanophosphor coated glass, line (b), on a glass substrate was ~65% in the spectral range of 400–700 nm. Eu^{2+}-activated CMS nanophosphors dispersed coating solution for fabricating transparent luminescent layers was prepared by dispersing 0.05 wt% of CMS nanophosphors in 2-methoxyethanol-based solvent. By using the controlled nanophosphors, the emissive and highly transparent luminescent layers can be realized, resulting in plasma discharge-operated transparent display devices.

Finally, a transparent PDP panel for plasma discharge was fabricated. The test panel consisted of $6 \times 9\ cm^2$ size front and rear glass plates. Glass plate coated with multilayer ITO conducting electrodes, dielectric layer, and MgO film were coated on the front plate. The phosphor layer on the rear glass plate contained as-prepared Eu^{2+}-doped CMS nanophosphors made by spin-casting followed by post annealing. Schematic drawing of the device structure and layer dimensions are shown in Fig. 6(a).

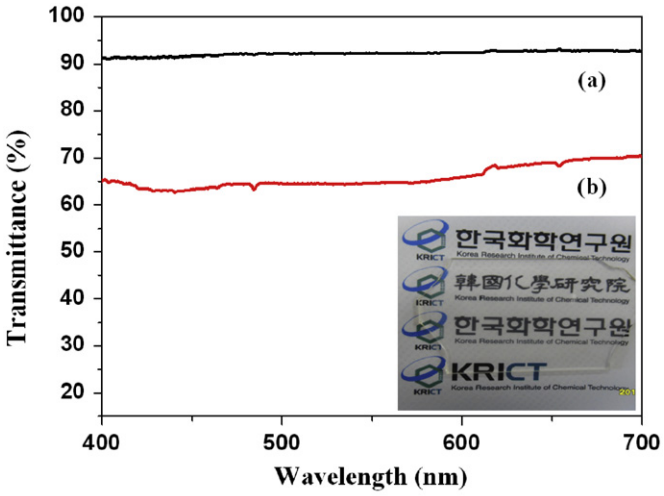

Fig. 5. UV–visible transmittance of the (a) bare glass and (b) particles coated layer. Inset image is the photograph of phosphor coated glass substrate.

Upon a plasma discharge condition with an AC-driven 290 V pulse voltage, the test panel without a nanophosphor layer under gas discharge exhibits a blue-reddish emission due to the radiative relaxation of excited Xe/Ne mixture gases, as shown in Fig. 6(b) of "Without phosphor". For the nanophosphor coated panel (noted as "With phosphor"), the characteristic blue emission emitted from the phosphor layer, as well as the plasma radiation, was clearly observed. The phosphor layer was only excited by the VUV produced from the gas mixtures during the plasma discharge, whereas visible light was produced from the VUV stimulation of the phosphor layer. The mixture gas-related reddish emission was completely screened by a strong blue emission from the Eu^{2+}-doped CMS nanophosphors. Indeed, completely dispersed nanoparticles were not obtained because of the sintering between particles, as shown in Fig. 2(a). Nevertheless, the results obtained suggest that the reverse micelle method we proposed may be a useful route for preparing fine CMS phosphor particles and phosphor layers.

Both measured emission spectra were presented in Fig. 6(c). The emission spectrum of the nanophosphors coated PDP panel was almost identical to that of the measured in particle, as shown in Fig. 3(b). The luminance of a nanophosphor coated panel was 40 cd/m^2, while the luminance of the bare glass plates was below 5 cd/m^2.

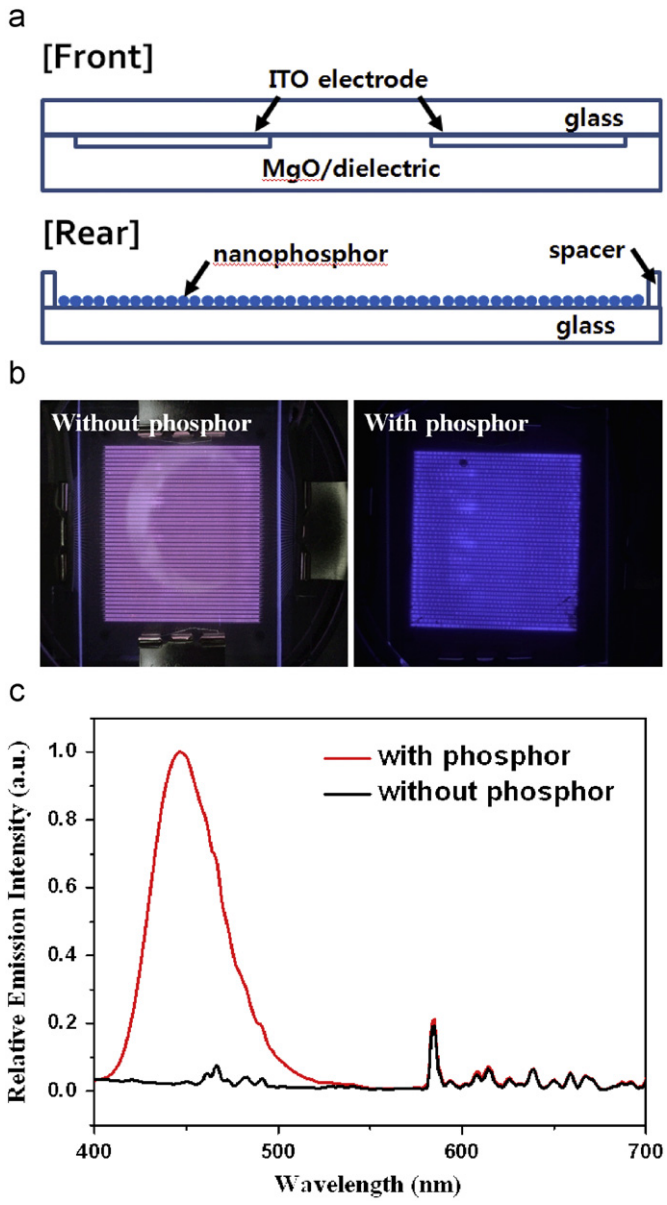

Fig. 6. (a) Schematic diagram of a mini-sized plasma discharge panel we made. (b) Photographs of the bare glass (left) and phosphor coated layer (right) under Xe/Ne gas discharge. (c) Corresponding emission spectra.

4. Conclusions

Eu^{2+} doped CMS nanophosphor particles were prepared by using a reverse micelle method, followed by calcinations in air and reducing ambient. It was found that the as-prepared Eu^{2+} activated CMS particles showed strong blue emission induced by the allowed $4f$–$5d$ transition of Eu^{2+} ion, similar to that of the micronscale phosphor synthesized by a conventional solid-state reactions. The luminescence decay of the corresponding nanophosphors fits well into a single-exponential behavior, which means the activators, Eu^{2+} ions, are properly substituted followed by blue emission in reverse micellar grown CMS nanoparticles absent from the surface defect induced non-radiative transition. By using the controlled nanophosphors followed by the spin-casting method, the emissive and transparent luminescent layers in plasma discharge-driven display devices can be realized even though the emission intensity was still low. This work demonstrates the feasibility of the nanophosphor-coated luminescent layers as a facile route to achieve upcoming transparent emissive devices such as transparent PDPs.

Acknowledgments

The authors are grateful to Dr. Yong-Seog Kim and his colleagues for the help in characterizing the luminescent properties of film layers under plasma discharge conditions. This research was supported by a grant (F0004073-2010-33) from the Information Display R&D Center, one of the Knowledge Economy Frontier R&D programs funded by the Ministry of Knowledge Economy of the Korean government.

References

[1] Y.A. Ono, Electroluminescent Displays, World Scientific Publishing Company, Singapore, 1995.
[2] Y.W. Song, K.H. Hwang, S.G. Yoon, J.H. Ha, K.N. Kim, J.H. Lee, S.C. Kim, SID Symp. Dig. 41 (2010) 144–147.
[3] J.P. Boeuf, J. Phys. D: Appl. Phys 36 (2003) R53–R79.
[4] T. Jüstel, H. Nikol, Adv. Mater. 12 (2000) 527–530.
[5] C. Feldmann, T. Justel, C.R. Ronda, P.J. Schmidt, Adv. Funct. Mater. 13 (2003) 511–516.
[6] A. Konrad, U. Herr, R. Tidecks, J. Appl. Phys. 90 (2001) 3516–3523.
[7] G. Buhler, C. Feldmann, Appl. Phys. A 87 (2007) 631–636.
[8] W.S. Song, H.N. Choi, Y.S. Kim, H.S. Yang, J. Mater. Chem. 20 (2010) 6929–6934.
[9] C. Liu, B. Zou, A.J. Rondinone, Z.J. Zhang, J. Phys. Chem. B 104 (2000) 1141–1145.
[10] T. Hirai, Y. Asada, I. Komasawa, J. Colloid Interface Sci. 276 (2004) 339–345.
[11] Y. Wu, S. Bose, Langmuir 21 (2005) 3232–3234.
[12] T. Kunimoto, R. Yoshimatsu, K. Ohmi, S. Tanaka, H. Kobayashi, IEICE Trans. Electron. E85-C (2002) 1888–1894.
[13] S. Oshio, T. Matsuoka, S. Tanaka, H. Kobayashi, J. Electrochem. Soc. 145 (1998) 3903–3907.
[14] K. Yokota, S.X. Zhang, K. Kimura, J. Lumin. 92 (2001) 223–227.
[15] L. Jiang, C. Chang, D. Mao, J. Alloys Compd. 360 (2003) 193–197.
[16] T. Kida, M.M. Rahman, M. Nagano, J. Am. Ceram. Soc. 89 (2006) 1492–1498.
[17] L. Jiang, C. Chang, D. Mao, C. Feng, J. Alloys Compd. 377 (2004) 211–215.
[18] K.Y. Jung, K.H. Han, Y.C. Kang, H.K. Jung, Mater. Chem. Phys. 98 (2006) 330–336.
[19] S. Hosokawa, Y. Tanaka, S. Iwamoto, M. Inoue, J. Mater. Sci. 43 (2008) 2276–2285.
[20] D.S. Zang, J.H. Song, D.H. Park, Y.C. Kim, D.H. Yoon, J. Lumin. 129 (2009) 1088–1093.
[21] J. Shan, M. Uddi, N. Yao, Y. Ju, Adv. Funct. Mater. 20 (2010) 3530–3537.
[22] X. Bai, H. Song, L. Yu, L. Yang, Z. Liu, G. Pan, S. Lu, X. Ren, Y. Lei, L. Fan, J. Phys. Chem. B 109 (2005) 15236–15242.